Structure of the Transmembrane Signal Initiation Site of the Relaxin-Like Factor (RLF/INSL3)†

Erika E. Büllesbach and Christian Schwabe*

Department of Biochemistry and Molecular Biology, Medical University of South Carolina, 173 Ashley Avenue, Charleston, South Carolina 29425

Received April 15, 2007; Revised Manuscript Received June 13, 2007

ABSTRACT: We have discovered the signal initiation structure of the relaxin-like factor and shown its function to be independent of the amino acid side chains in the contact region. Evidence presented in this article suggests that signal induction is a function of the peptide bond and that completion of the signaling contact is initiated by ligand binding to the leucine-rich repeat G-protein coupled receptor 8 (LGR8). The specific mode of binding forces certain peptide bonds into a signaling position. This observation implies that the receiving structures are equally nonspecific so that signaling should occur at any peptide bond of the receptor or the trans-membrane loop that is within reach of the signaling wires of the receptor-bound ligand. Our observations offer an explanation for ligand cross-talk as well as for the ability of some antibodies to elicit the biological response normally associated with a specific ligand.

The homeostatic control of macro-organisms depends largely upon a number of circulating hormones and their receptors. According to the prevailing and highly successful paradigm, the specificity of the system is the result of selective hormone/receptor interaction. Receptor structures have received a great deal of attention from protein chemists and X-ray crystallographers, whereas the actual generation and the nature of the signal that would travel through the cell membrane and connect the homeostatic controls to the vast network of intracellular response elements has remained enigmatic. The experimental results presented in this article suggest strongly that the initiation of the last extra-cellular step is associated with the peptide bond and is independent of the side chains of the involved amino acids.

Normal testicular descent in human infants is, to a significant part, dependent upon the relaxin-like factor (RLF[1]) (*1*−*3*), also named insl3. The action of RLF is exerted though the leucine-rich repeat G-protein-coupled receptor 8 (LGR8/great) (*4*, *5*). We have chemically synthesized RLF (*6*, *7*) as well as all of the alanine derivatives that were used to search for the receptor-binding (*8*) and the signal initiation sites (*9*). As a result, we know that receptor binding is a function of the B-chain exclusively (*8*, *10*, *11*) and specifically that the residues at the N-termini of both chains do not contribute significantly to the binding energy (*8*, *9*).

In this article, we describe that signal activation in contrast to LGR8 binding is independent of the amino acid composition but requires both N-terminal chains in some form. The observation that modification within the N-terminal regions of the A- and B-chains did not significantly influence receptor binding made it possible to explore the structure of the signal initiation site using cAMP production as the readily quantifiable endpoint.

MATERIALS AND METHODS

Peptide Synthesis. RLF and derivatives were synthesized by solid-phase techniques in combination with our site-directed sequential disulfide bond formation as published in detail elsewhere (*7*, *9*). *N*-methylalanine was incorporated using the protocol published by Biron et al. (*12*).

DesA(1−*4)N(α)-acetyl-Lys(A5) amide(A26) RLF and the Corresponding Lys(εA5)-Asp(βA19) Cross-Linked hRLF Derivative*. Human RLF A-chain was synthesized on Knorr resin (Advanced ChemTech, Louisville, KY) using standard Fmoc chemistry with the appropriate differential protecting groups for the four cysteines (trityl in positions A10 and A15, acetamidomethyl in position A11, and tertiary butyl in position A24) (*7*, *9*). Fmoc-Lys(Boc) was introduced in position A5, the Fmoc group removed by piperidine treatment, and the N-terminus acetylated with a 10-fold excess of acetic anhydride in dimethylformamide for 60 min at ambient temperature. Thereafter, the peptide was partially deprotected using a TFA-scavenger cocktail (*13*) for 2 h at room temperature. The peptide was precipitated with ice-cold ether and the pellet collected by centrifugation. The peptide was air-dried, dissolved in 50% acetic acid (∼10 mg/mL; 4 μM) and the free cysteines in positions A10 and A15 oxidized by titration with iodine in acetic acid. The reaction mixture was diluted to 20% acetic acid with water and the intra-A-chain disulfide product isolated by preparative HPLC. A portion of the product (8.9 μmol) was

† This work was supported by Grant 1-R01-HD40406 from the National Institutes of Health and by the Medical University of South Carolina, Charleston University Research Committee.

* To whom correspondence should be addressed. Tel: 843-792-9929. Fax: 843-792-4850. E-mail: schwabec@musc.edu.

[1] Abbreviations: 293T, human embryonic kidney cell line; DMEM, Dulbecco's modified essential medium; EDTA, ethylenediaminetetraacetate; Fmoc, 9-fluorenylmethyloxycarbonyl; HPLC, high performance liquid chromatography; LGR8, leucine-rich repeat G-protein coupled receptor 8; MALDI-TOF-MS, matrix assisted laser desorption/ionization time-of-flight mass spectrometry; MeAla, *N*-methylalanine; RLF, relaxin-like factor; TFA, trifluoroacetic acid; Tris, tris(hydroxymethyl)aminomethane.

10.1021/bi700708s CCC: $37.00
Published on Web 08/03/2007

dissolved in 300 μL of dimethylformamide, and the side chains of Lys(A5) and Asp(A19) were condensed using 5 equiv of benzotriazolyloxy-tris[pyrrolidino]-phosphonium hexafluorophosphate (PyBop) and 5 equiv of diisopropylethylamine for 40 min at room temperature. The reaction was diluted with 9 volumes of 0.1% TFA in water and purified by preparative reversed-phase HPLC.

Side by side, the cross-linked A-chain and its open precursor were combined with an equivalent amount of B-chain by site-directed disulfide synthesis, which includes the specific deprotection/activation of cysteine A24, the combination with mono-thiol B-chain carrying an acetamidomethyl protecting group in position B10 and a sulfoxide group in methionine B5, oxidative deprotection of the acetamidomethyl groups under formation of the third disulfide bond, and selective reduction of the methionine sulfoxide to yield the corresponding RLF analogue (*7*, *9*). The yield based on the initial HPLC-purified chains was 25.9% (MALDI-MS: *m*/*z* 6034.1 (calcd 6034.1)) for the open derivative and 31.1% (MALDI-MS: *m*/*z* 6015.2 (calcd 6016.1)) for the closed (cross-linked) derivative.

A1,B9-des(B1−8)-bis-acetyl-hRLF. Synthetic desB(1−8)-hRLF (1 mg, 200 nmol) was dissolved in 1 mL of water followed by 200 μL of 0.25 M sodium phosphate buffer at pH 7.5. Three equivalents of acetic anhydride (600 nmol) in 0.42 mL of tetrahydrofuran was added and the reaction stirred for 30 min at room temperature, quenched with 1 mL of 1% TFA in water, and left for 1 h at room temperature before purification by reversed-phase HPLC on a C_{18} column. Yield: 160 μg (16%) (MALDI-MS: *m*/*z* 5408.9 (calcd 5410.2)).

RLF Stock Solution. The corresponding RLF derivative (∼0.5 mg/mL) was dissolved in water, and the protein content was determined accurately by UV spectroscopy, using calculated absorbance coefficients (*14*). This stock solution was used for all subsequent tests.

Chromatography. All products were analyzed by HPLC in two different systems. The solvents, identical in both systems, consisted of 0.1% TFA in water (solvent A) and 0.1% TFA in 80% acetonitrile (solvent B). System 1 consisted of a Bakerbond wide-pore C_{18} column (4.1 mm × 250 mm) in combination with a 30 min linear gradient from 20% to 60% B, a flow rate of 1 mL/min, and UV detection of the effluent at 220 nm. System 2 consisted of an Aquapore 300 C_8 column (2.1 mm × 30 mm) in combination with a 60 min linear gradient from 20 to 60% B, a flow rate of 100 μL/min, and UV detection of the effluent at 230 nm.

Reduction and Chain Separation. The RLF derivative (10 μg) was reduced in 25 mM dithiothreitol in 0.1 M Tris/HCl at pH 8.6 containing 3 M guanidinium chloride for 30 min at 37 °C. The reduction was quenched with 5 μL of glacial acetic acid and injected onto an Aquapore 300 column (system 2).

Enzymatic Digest and Peptide Mapping. RLF analogues (5 μg) in 50 mM phosphate buffer at pH 7.5 (final volume, 10 μL) was digested with staphylococcus V8 protease (enzyme to substrate ratio, 1:10 by weight) for 16 h at 25 °C (*15*), followed by trypsin (enzyme to substrate ratio 1:20 by weight) for 30 min at 37 °C. The reaction was quenched by the addition of 50 μL of 0.1% TFA in water, and peptides were analyzed by MALDI-TOF MS.

Matrix-Assisted Laser Desorption/Ionization Time-of-Flight Mass Spectrometry (MALDI-TOF MS). MALDI-TOF MS was performed at the mass spectrometry facility at the Medical University of South Carolina, Charleston. The RLF analogue (1 μg), dissolved in 1 μL of 0.1% TFA or 1 μL of the enzymatic digest, was mixed with 3 μL of α-cyano-4-hydroxycinnamic acid (50 mM in acetonitrile/water 4/1 v/v), and 1 μL was spotted on a sample plate. Mass spectra were acquired on an Applied Biosystems (ABI) Voyager DR-STE instrument in the linear mode.

Vectors and Cell Lines. LGR8 was cloned into the pcDNA3.1.zeo plasmid (*5*), kindly supplied by Dr. Hsueh, Department of Obstetrics and Gynecology, Stanford University School of Medicine. The receptor was expressed in the human embryo kidney cell line 293T/17, procured from the American Type Culture Collection (ATCC CRL-11286).

Cell Culture. Cells (293T/17) stably transfected with LGR8-pcDNA3.1.zeo expressing 8700 receptors/cell (*9*) were used between passage 20 and 70. Cells were cultured in Dulbeccos modified Eagles medium (DMEM) containing 4.5 g/L glucose, L-glutamine, and 110 mg/L sodium pyruvate (Gibco, Invitrogen, Carlsbad, CA) and further supplemented with 10% fetal bovine serum (Atlanta Biologicals, Lawrenceville, GA), 100 international units/mL penicillin, 100 μg/mL streptomycin, and 400 μg/mL zeocin (Invivogen, San Diego, CA), in a water-saturated atmosphere containing 5% CO_2 at 37 °C. Cells were detached with trypsin/EDTA (Gibco, Invitrogen, Carlsbad, CA) and 10^7 cells used to seed 75 cm^2 culture flasks.

Competitive Receptor-Binding Assays. Stably transfected 293T/17 cells were grown to 80% confluence and then dislodged with 0.5 M EDTA (pH 7.5) (1 mL/10 mL of conditioned medium) for 10 min at 37 °C. Cells were collected by centrifugation at 2000*g* for 10 min, suspended 2 times in 1 mL ice cold binding buffer (20 mM Hepes at pH 7.5, 1% bovine serum albumin, 0.1 mg/mL lysine, 1.5 mM $CaCl_2$, 50 mM NaCl, and 0.01% NaN_3), and recentrifuged at 4 °C for 10 min at 2000*g*. In 100 μL of binding buffer, 10^6 cells were treated with 25 fmol (100,000 cpm) ^{125}I-Tyr(A9) hRLF (*16*) in the presence of varying concentrations of hRLF or hRLF derivatives for 60 min at room temperature. Thereafter, the cells were diluted with 1 mL of ice-cold binding-buffer and collected by centrifugation (10 min at 2000*g* at 4 °C). The pellet was washed with 1 mL of the same buffer and centrifuged for 10 min at 5000*g* at 4 °C. The tips of the vials containing the pellets were placed in counting tubes and transferred to a gamma counter for analysis. Total binding was determined in the absence of and nonspecific binding in the presence of 32 pmol of unlabeled RLF. In a regular assay, total binding produced approximately 30,000 cpm and nonspecific binding less than 5% of the total binding. Data of at least three independent binding assays were pooled and presented as the mean (±SEM).

Cyclic AMP Assay. Stably transfected LGR8-293T/17 cells were seeded in 24-well tissue culture plates with 250,000 cells/well and grown in 500 μL of DMEM, supplemented with fetal bovine serum (10%) and antibiotics. Twenty-four hours later, the conditioned medium was replaced by 100 μL of 3-isobutyl-1-methylxanthine (5 mM) in DMEM containing 1% bovine serum albumin. The cells were incubated for 1 h at 37 °C in 5% CO_2 before 100 μL of

Table 1: MALDI Mass Spectrometry Data of RLF Derivatives of the Intact Molecule and the Cystine Containing Fragments after Endoprotease GluC/Tryptic Cleavage

	intact	N-terminal[a]		C-terminal[b]
derivative	*m/z* found (calcd)	*m/z* found (calcd)	segment	*m/z* found (calcd)
hRLF	6293.1 (6293.2)	2188.1 (2185.5)	A9−19/B9−16	1410.1 (1408.7)
K5 open	6034.1 (6034.1)	2184.7 (2185.5)	A9−19/B9−16	1407.9 (1407.7)
K5D19 closed[c]	6015.2 (6016.1)	N/A	N/A	N/A
MeAla(A8)	6222.8 (6222.2)	2767.3 (2767.2)	A1−19/B9−16	1408.0 (1408.7)
MeAla(A9)	6215.9 (6215.2)	2859.0 (2760.1)	A1−19/B9−16	1408.2 (1408.7)
D-Pro(A9)	6229.2 (6227.2)	2869.9 (2868.2)	A1−19/B9−16	1406.1 (1408.7)
desB(1−6)	5583.5 (5581.4)	2184.1 (2185.5)	A9−19/B9−16	1406.8 (1408.7)
desB(1−7)	5454.7 (5452.3)	2183.4 (2185.5)	A9−19/B9−16	1407.7 (1408.7)
desB(1−8)	5326.0 (5324.2)	2187.5 (2185.5)	A9−19/B9−16	1409.7 (1408.7)
AcdesB(1−8)	5410.2 (5408.2)	2229.6 (2228.5)	A9−19/AcB9−16	1409.8 (1408.7)
D-Pro(B9)	6280.0 (6277.2)	2425.0 (2422.7)	A9−19/B6−16	1406.0 (1408.7)

[a] N-terminal cystine-containing fragment varies with the modification. [b] C-terminal cysteine fragment is identical for all RLF derivatives, except for K5 (open), which is C-terminally amidated. [c] The intra-chain isopeptide bond involves Asp(A19) and prevents cleavage within the A chain.

hormone dilution, prepared in the same buffer, was added. The cultures were grown at 37 °C in 5% CO_2 in air for 16 h. Thereafter, the plates were moved into a −80 °C freezer and kept at least for 6 h. Prior to the assay, 20 μL of 0.5 M EDTA was added to each well, the plate incubated for 15 min at 37 °C, the contents transferred into 1.5 mL bullet tubes, and heated to >90 °C for 10 min in a water bath. Cell debris was removed by centrifugation at 14,000 rpm for 10 min at 4 °C. The supernatant (100 μL) was reacted with acetic anhydride and the 2′-O-acyl-cAMP concentration determined by radioimmunoassay using [^{125}I]-succinyl-cAMP-tyrosyl methyl ester (*17*) (20,000 cpm = 5 fmol) and anti-cAMP antiserum (Chemicon, Temecula, CA). Total response was determined in the presence of 80 pmol of human RLF and nonspecific response was determined in the absence of RLF. Assays of hRLF derivatives were compared with human RLF standards run in parallel. Assays were performed in duplicate, and three independent assays were averaged (±SEM).

RESULTS AND DISCUSSION

To characterize the mechanism of LGR8 activation by RLF, we generated RLF derivatives with modifications in the N-terminal segments. The proteins were produced by solid-phase synthesis of the two chains and their subsequent combination by the directed synthesis of the three disulfides (*7*, *9*). All RLF derivatives were homogeneous in two analytical HPLC systems, and upon reduction, two polypeptide chains were observed by HPLC. MALDI-TOF MS showed the expected mass/charge ratio (Table 1). To prove the correct orientation of the A- and B-chains, enzymatic digests with endopeptidase Glu-C and trypsin were conducted. Hydrolysis at Asp(A19) in the A-chain and Arg(B16) and/or Arg(B20) in the B-chain is required for the separation of the two cystine-containing domains. The C-terminal disulfide peptide A20−26/B21−26 was detected in all derivatives except the intra-A-chain cross-linked derivative (Figure 1B), where Asp(A19) is part of the intrachain isopeptide bond. The mass/charge ratio of the N-terminal cystine-containing fragment corresponded to the introduced modification.

The first experimental series consisted largely of N-terminal A-chain truncations (*9*). Deletion of residues A(1−9) did not attenuate receptor binding but essentially abolished cAMP production. Adding a stochiometric amount of the free peptide A(1−9) did not restore cAMP synthesis. DesA(1−8) RLF was in fact a perfect inhibitor of RLF function called RLFi. The inhibition and binding curves intersected exactly at 2 ng/mL, which is the IC_{50} of RLF (*9*).

This finding offered the first opportunity to study a *bona fide* signal initiation structure. Sequential removal of N-terminal A-chain residues or substitution with alanine should bring signaling to an abrupt halt when the critical residue has been removed or substituted. Instead, we noticed that cAMP production diminished progressively as the A-chain was shortened but that replacement of Arg(A8) or Tyr(A9) with alanine did not perturb the signaling activity of LGR8 (*9*). This observation suggested that there is no distinct signaling residue in the part of RLF that was essential for signaling. The fact that mouse and rat RLF are active (*18*, *19*) although the sequence A6−9 (AVHR) differs from the human sequence (PARY) in every position (*20*−*22*) is consistent with this result.

What would be the size and nature of the contact region, and where would it be? The common feature in all peptide chains is the double bond character of the backbone amide, and if that were the immediate contact, leaving the chain intact but bending the primary structure out of place should disable signal transmission. Thus, we replaced Tyr(A9) with D-Pro, and this modification had no effect on receptor binding while signal initiation was severely disturbed (Figure 1). The mere presence of a peptide chain in a defined position provided the structural requirement for signaling, whereas preventing the chain from assuming that position in space abolished signal initiation. This in turn suggested two equally exciting possibilities, namely, that the chain had to be able to move into a certain position in order to complete the signal initiation cycle and that the electron configuration of the peptide bonds may be the actual initiators of the signaling sequence that traveled to the cell interior. With D-proline in position A9, the tail of the A-chain could not make contact with the peptide bond of the signal recipient.

Addressing the effect of chain mobility on signaling, an intra A-chain cross-link was introduced between A5 and A19 of RLF. The RLF A-chain was synthesized with asparagine in position A5 replaced by lysine, shortened by four residues,

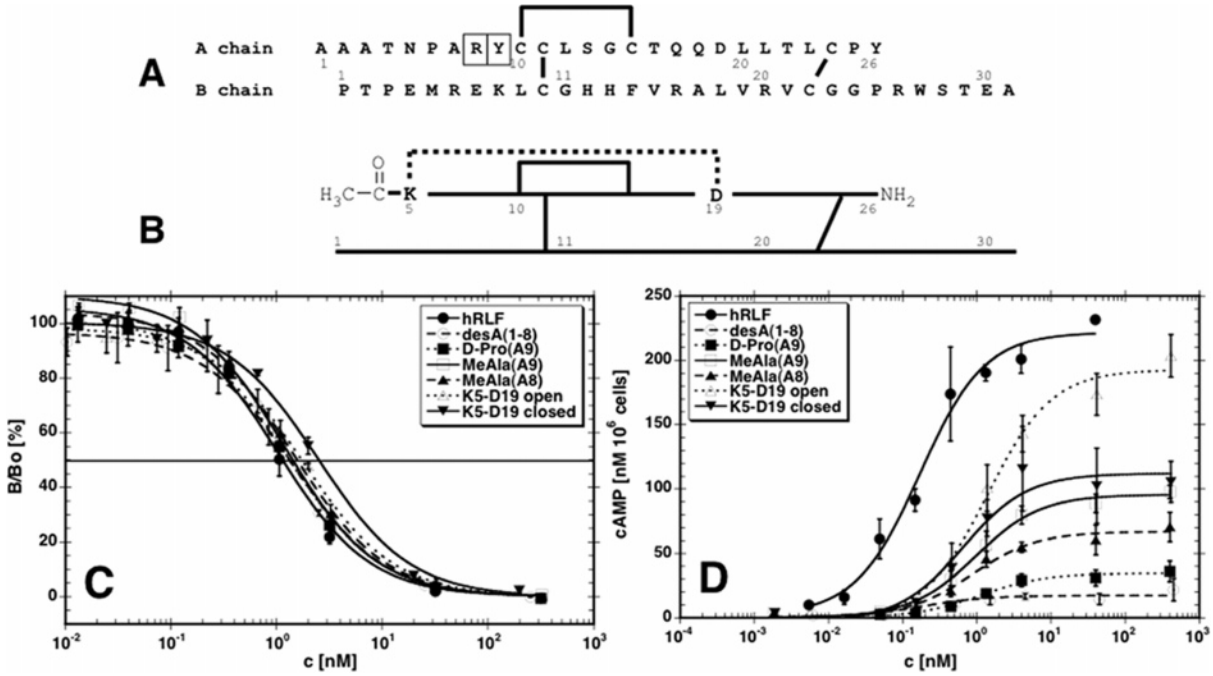

FIGURE 1: Human RLF derivatives with modifications in the A-chain. (A) Sequence of human RLF. The squares highlight the residues modified in the present study. (B) Structure of the intra-A-chain cross-linked RLF. The dashed line indicates the position of the cross-linked, closed, structure. The non-cross-linked, open, structure served as control. The A-chain is N-terminally truncated by four residues, N-acetylated, and amidated at the C terminus. (C) Competitive receptor-binding assays using ^{125}I-Tyr(A9)-labeled hRLF tracer in combination with 293T cells stably transfected with LGR8. For each derivative, three independent experiments were conducted, and for each experiment, an hRLF standard was run in parallel. The data were pooled, and the mean of each set of measurements (±SEM) is presented. The graph includes previously reported data of desA(1−8) hRLF (*9*). (D) RLF-stimulated accumulation of cAMP was measured using stably transfected LGR8 293T cells as described. For each derivative, three independent assays were performed with hRLF run in parallel. Data were normalized on the hRLF standard, pooled, and the mean (±SEM) presented.

acetylated at the N-terminus, and the C terminus amidated. The open structure retained full LGR8 binding and caused maximum accumulation of cAMP, albeit at a 10-fold higher EC_{50}. When the isopeptide bond was established between the side chains of lysine (A5) and aspartic acid (A19), only a small effect on binding avidity was observed, but maximum cAMP production was reduced by 50% (Figure 1D).

Could one modify the character of the peptide bond such that the electronic configuration is no longer sufficient to initiate signaling? Working with the full length RLF, we introduced N-methyl alanine into position 8 and measured receptor binding as well as cAMP production. Receptor binding was unaffected, while cAMP production was severely curtailed. Placing an N-methyl alanine into position A9 also showed significant reduction in signaling activity. Clearly, signal initiation is attenuated if the contiguity of the peptide bond configuration is interrupted. From these observations, it appears that the major signal-activating moiety is the peptide bond of amino acids A8 and A9, in particular their hydrogen donating feature. The 3D solution structure of RLF shows that residues A7 to A15 form an α helix (*11*). N-methylation in positions A8 and A9 does not compromise the helix since the residues are located on the N-terminal turn, and in this location, there are no $C_i{=}O\cdots\cdots HN_{i+4}$ hydrogen bonds. Therefore in native RLF, the secondary amide nitrogen can interact with positions on the receptor causing a shift in polarity across the lipid bilayer, while the tertiary amide nitrogen cannot. The perturbations caused by N-methylation (Figure S1, Supporting Information) are comparatively minor and difficult to interpret when some full agonists show a much more disturbed CD profile (*8*).

How extensive is the signal initiation structure of RLF? When we examined the N-terminal end of the B-chain of RLF, it quickly became clear that with the A-chain intact, one could delete 6 or 7 residues from the N-terminal end of the B-chain without compromising the affinity of the derivatives for LGR8 (Figure 2). DesB(1−8) caused a 60% loss in binding avidity, and this reduction cannot be reversed by N-terminal acetylation. Cyclic AMP dose−response curves are identical to human RLF when six residues are removed from the N-terminus. The maximum cAMP accumulation dropped to 65% when seven residues were deleted and to about 20% when eight residues were deleted from the N-terminus of the B-chain. Acetylation of desB(1−8) improves cAMP production to the level of desB(1−7), suggesting again that the peptide bond character is important for signaling. Single replacements by alanine had a minimal effect on binding and none on cAMP production (*8*).

Introducing D-Pro in position B9 demonstrated that the relative position of the N-terminal B-chain is as important for signaling as it is for the A-chain. In fact B9 D-Pro RLF loses its ability to stimulate cAMP production completely while retaining 50% of the receptor-binding capacity (Figure 2). In addition, the CD spectrum revealed a disturbed structure lacking the α-helix signature of RLF (Figure S2, Supporting Information).

Close scrutiny of the 3D structure of RLF (Figure 3) discloses that the three peptide bonds on the A-chain segment A7−A9 are oriented such that the amide protons are exposed on the surface, while the carbonyl oxygens, hydrogen-bonded to the $i + 4$ NH of the second helix turn, are hidden. The

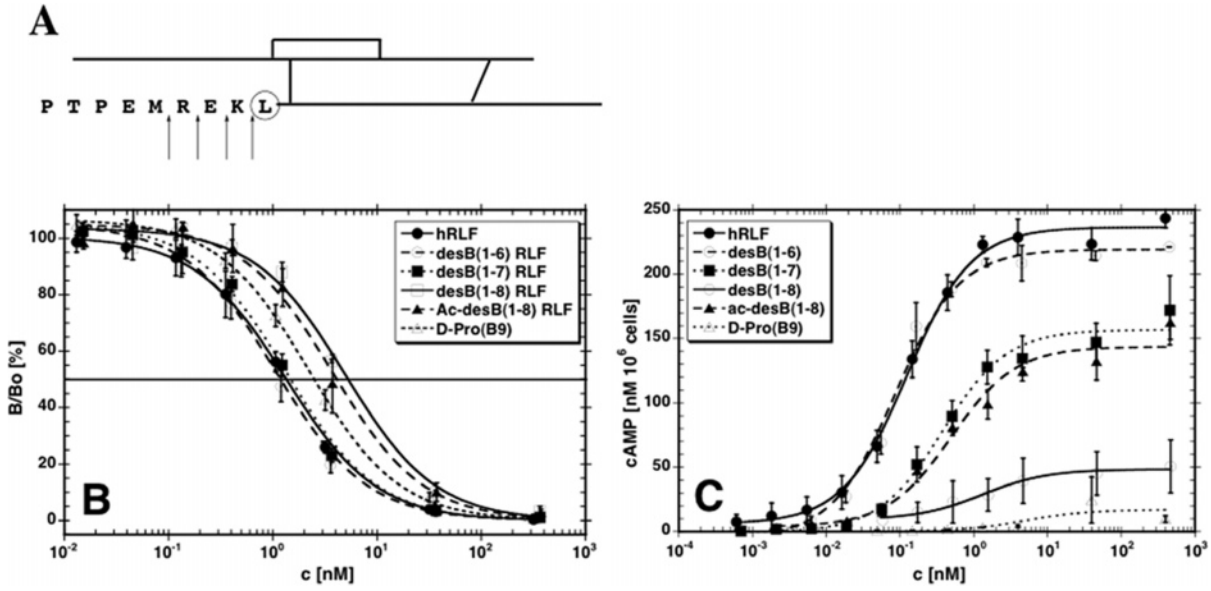

FIGURE 2: Human RLF derivatives with modifications in the B-chain. (A) Display of the N-terminal sequence B(1−9) in which the modified residue is circled and the truncations are designated by arrows. (B) Competitive receptor-binding assays using ^{125}I-Tyr(A9)-labeled hRLF as tracer and 293T cells stably transfected with LGR8. For each derivative, three independent experiments were conducted, and an hRLF standard was run in parallel. (C) RLF-stimulated accumulation of cAMP was measured using stably transfected LGR8 293T cells. For each derivative, three independent assays were performed with hRLF run in parallel. Data were standardized with hRLF and pooled, and the mean (±SEM) is presented.

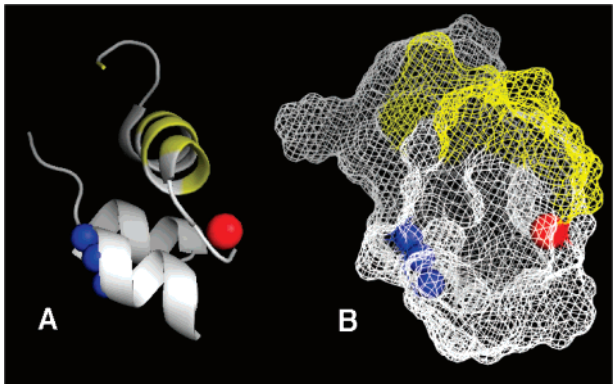

FIGURE 3: Presentation of the three-dimensional structure of RLF based on the NMR solution structure pdb 2h8b. Not displayed are the flexible regions A(1−4), B(1−6), and B(28−31). Three-amide hydrogens of the signaling site in the A-chain (A7−9) are exposed on the first turn of the N-terminal helix of the A-chain on the surface in a single cluster (blue spheres). Of the important amide bonds of the complementary signaling region between Lys(B8) and Leu-(B9), the carbonyl group of Lys(B8) is exposed on the surface (red sphere), while the NH of Leu(B9) (not shown) points to the interior of the molecule. (A) Ribbon presentation of the RLF. The blue spheres indicate the hydrogens of the amides Ala(A7), Arg(A8), Tyr(A9), the red sphere is the carbonyl oxygen of Lys(B8), and yellow indicates the LGR8 binding site. (B) Mesh presentation to show surface exposure and spatial separation of the signaling features of the A and B-chains. (This Figure was generated in PyMol).

critical peptide bond on the B-chain (B8 to B9) is oriented such that the carbonyl oxygen is exposed on the surface, while the NH is hidden. The critical regions of the A- and B-chains are located about 11−14 Å from each other (Figure 3). The discovery of a nearly complete separation of the binding and the signal initiation structures made it possible to investigate the signaling process directly.

A quasi insulator (the disulfide bond in positions A11 and B10) and the A-chain loop (A11−A15) separate the two hot wires (like in an electrical system) in RLF referring to positions 7−9 in the A- and B-chains. It is not known whether the two chains have to be in contact with the recipient peptide bond at the same time or sequentially, but it is clear is that both contacts have to be completed. At the present state of knowledge, one may speculate that an electronic push/pull might be propagated along one of the transmembrane segments through the lipid bilayer to create a G-protein binding site. A two-point contact could be made with one ecto loop or with two closely spaced ecto loops of the transmembrane segments of LGR8. Our results do not preclude the possibility that the C-terminal extension of the leucine-rich repeat domain wraps around the signaling region of RLF or that the signal is assisted by the N-terminal lipoprotein receptor class A domain (*23*) as it appears to be in the LGR7/relaxin pair.

Models involving conformational changes in the transmembrane portion, for example (*24*), require a certain energy input, and the peptide bond is perhaps the best if not the only candidate. The only other prospect would be binding energy, but that seems unlikely because the binding energy does not change significantly when the signaling portion of the molecule is deleted. It is most likely that the peptide bond once brought into the correct position by the specific binding of RLF to LGR8 is the initiator of signaling into the cell. Our observations also imply a mechanism for ligand cross-talk that has puzzled researchers for a long time and for the equally enigmatic signaling occasionally observed when antibodies against a receptor have developed inadvertently (*25*). One explanation is the lack of special structural requirements for signaling. The antibody specificity would cause binding on the receptor surface while putting peptide bonds in position such that they can reach the signaling structure and initiate the signal. Thus, antibody-mediated activation could lead to long activation cycles. The same considerations apply to cross-reacting ligands.

For decades research efforts have created a complex image of the extracellular receptor/ligand world and have began to put together what is already an even more complex world of intracellular response pathways. Their functional connection through as little as 20−30 Å, which has resisted inquiry for many years, is now coming into focus. This article, to the best of our knowledge, provides the first picture of the signal initiation site of a ligand.

ACKNOWLEDGMENT

We thank Robert Bracey and George Fullbright for their technical assistance.

SUPPORTING INFORMATION AVAILABLE

CD spectra of hRLF derivatives modified in the N-terminal region of the A- and B-chains. This material is available free of charge via the Internet at http://pubs.acs.org.

REFERENCES

1. Zimmermann, S., Steding, G., Emmen, J. M., Brinkmann, A. O., Nayernia, K., Holstein, A. F., Engel, W., and Adham, I. M. (1999) Targeted disruption of the Insl3 gene causes bilateral cryptorchidism, *Mol. Endocrinol. 13*, 681−691.
2. Nef, S., and Parada, L. F. (1999) Cryptorchidism in mice mutant for Insl3, *Nat. Genet. 22*, 295−299.
3. Hutson, J. M., and Hasthorpe, S. (2005) Abnormalities of testicular descent, *Cell. Tissue Res. 322*, 155−158.
4. Overbeek, P. A., Gorlov, I. P., Sutherland, R. W., Houston, J. B., Harrison, W. R., Boetther-Tong, H. L., Bishop, C. E., and Agoulnik, A. I. (2001) A transgenic insertion causing cryptorchidism in mice, *Genesis 30*, 26−35.
5. Kumagai, J., Hsu, S. Y., Matsumi, H., Roh, J. S., Fu, P., Wade, J. D., Bathgate, R. A. D., and Hsueh, A. J. W. (2002) InsL3/Leydig insulin-like peptide activates the LGR8 receptor important in testis descent, *J. Biol. Chem. 277*, 31283−31286.
6. Büllesbach, E. E., and Schwabe, C. (1995) A novel Leydig cell cDNA-derived protein is a relaxin-like factor (RLF), *J. Biol. Chem. 270*, 16011−16015.
7. Büllesbach, E. E., and Schwabe, C. (1999) Tryptophan B27 in the relaxin-like factor (RLF) is crucial for RLF receptor binding, *Biochemistry 38*, 3073−3078.
8. Büllesbach, E. E., and Schwabe, C. (2006) The mode of interaction of the relaxin-like factor (RLF) with the leucine-rich repeat G protein-activated receptor 8, *J. Biol. Chem.* 26136−26143.
9. Büllesbach, E. E., and Schwabe, C. (2005) LGR8 signal activation by the relaxin-like factor, *J. Biol. Chem. 280*, 14586−14590.
10. Del Borgo, M. P., Hughes, R. A., Bathgate, R. A., Lin, F., Kawamura, K., and Wade, J. D. (2006) Analogs of insulin-like peptide 3 (INSL3) B-chain are LGR8 antagonists in vitro and in vivo, *J. Biol. Chem. 281*, 13068−13074.
11. Rosengren, K. J., Zhang, S., Lin, F., Daly, N. L., Scott, D. J., Hughes, R. A., Bathgate, R. A., Craik, D. J., and Wade, J. D. (2006) Solution structure and characterization of the receptor binding surface of insulin-like peptide 3, *J. Biol. Chem.* 28287−28295.
12. Biron, E., Chatterjee, J., and Kessler, H. (2006) Optimized selective N-methylation of peptides on solid support, *J. Peptide Sci. 12*, 213−219.
13. King, D. S., Fields, C. G., and Fields, G. B. (1990) A cleavage method which minimizes side reactions following Fmoc solid phase peptide synthesis, *Int. J. Peptide Protein Res. 36*, 255−266.
14. Gill, S. C., and von Hippel, P. H. (1989) Calculation of protein extinction coefficients from amino acid sequence data, *Anal. Biochem. 182*, 319−326.
15. Drapeau, G. R. (1977) Cleavage at glutamic acid with staphylococcal protease, *Methods. Enzymol. 47*, 189−191.
16. Büllesbach, E. E., and Schwabe, C. (1999) Specific, high-affinity relaxin-like factor receptors, *J. Biol. Chem. 274*, 22354−22358.
17. Steiner, A. L. (1979) Cyclic AMP and Cyclic GMP, in *Methods of Hormone Radioimmunoassay* (Jaffe, B. M., and Behrman, H. R., Eds.) pp 3−17, Academic Press, New York.
18. Adham, I. M., Steding, G., Thamm, T., Büllesbach, E. E., Schwabe, C., Paprotta, I., and Engel, W. (2002) The overexpression of the INSL3 in female mice causes descent of the ovaries, *Mol. Endocrinol. 16*, 244−252.
19. Bogatcheva, N. V., Truong, A., Feng, S., Engel, W., Adham, I. M., and Agoulnik, A. I. (2003) GREAT/LGR8 is the only receptor for insulin-like 3 peptide, *Mol. Endocrinol. 17*, 2639−2646.
20. Koskimies, P., Spiess, A. N., Lahti, P., Huhtaniemi, I., and Ivell, R. (1997) The mouse relaxin-like factor gene and its promoter are located within the 3′region of the JAC3 genomic sequence. *FEBS Lett. 419*, 186−190.
21. Zimmermann, S., Schottler, P., Engel, W., and Adham, I. M. (1997) Mouse Leydig insulin-like (Ley I-L) gene: structure and expression during testis and ovary development, *Mol. Reprod. Dev. 47*, 30−38.
22. Spiess, A. N., Balvert, M., Tena-Sempere, M., Huhtaniemi, I., Parry, L., and Ivell, R. (1999) Structure and expression of the rat relaxin-like factor (RLF) gene, *Mol. Reprod. Dev. 54*, 319−325.
23. Hopkins, E. J., Layfield, S., Ferraro, T., Bathgate, R. A. D., and Gooley, P. R. (2007) The NMR solution structure of the relaxin (rxfp1) receptor lipoprotein receptor class a module and identification of key residues in the N-terminal region of the module that mediate receptor activation, *J. Biol. Chem. 282*, 4172−4184.
24. Ottemann, K. M., Xiao, W., Shin, Y. K., and Koshland, D. E., Jr. (1999) A piston model for transmembrane signaling of the aspartate receptor, *Science 285*, 1751−1754.
25. Jacobs, S., Chang, K. J., and Cuatrecasas, P. (1978) Antibodies to purified insulin receptor have insulin-like activity, *Science 200*, 1283−1284.

BI700708S